



## Survey of hydrogeological moving deformation of abandoned mine and numerical simulation of environmental control in collapse area

Zhengzhen An<sup>a</sup>, Yue Zhao<sup>a,b</sup>, Jun Wang<sup>b</sup>, Xuguang Li<sup>c,\*</sup>, Yanfei Zhang<sup>a,c</sup>

<sup>a</sup>Mining College of Liaoning Technical University, Fuxin 123000, Liaoning, China

<sup>b</sup>Institute of Innovation and Development for Fuxin Transition, Liaoning Technical University, Fuxin 123000, Liaoning, China

<sup>c</sup>Shenyang Geological Survey Center, China Geological Survey, Shenyang 110034, Liaoning, China, email: lixuguangsfsc@yeah.net

Received 20 August 2021; Accepted 23 September 2021

---

### ABSTRACT

The hydrogeological movement and deformation caused by the abandoned mine settlement area have a significant impact on the mine construction and ecological environment. The hydrogeological movement and ecological environmental governance in the region have certain importance. On the basis of consulting a large number of literature and on-site investigation, the deformation of the hydrogeological geology of the sedimentation area is studied by surface monitoring and numerical simulation. Fuzzy mathematics method is used to carry out the environmental impact assessment of abandoned land mines from the mine hydrogeological environmental environment and geological disaster distribution density. The monitoring results show that there is almost no change in mine levels in this region, and the maximum cumulative offset of X coordinates is -27 mm; the maximum accumulation displacement of Y coordinates is -35 mm; the maximum cumulative settlement of Z coordinate is -13 mm. The simulation results of the fast Lagrange analysis of the Continua (FLAC3D) software show that the maximum displacement of the X forward is 0.168 meters, and the maximum displacement in the X negative direction is -0.197 m. The evaluation results show that the mine area has a slight impact about 219.14 km<sup>2</sup>, the more severe the area of about 53.78 km<sup>2</sup>. This indicates that the settlement of the mine tends to be stable, the horizontal movement is relatively active; the surface can form a depressed basin; most of the mines in the region have a slight effect on the area, the main environmental problems are open-pit and damaged mountains. On the basis of environmental impact assessment, environmental protection and ecological repair countermeasures were proposed for the hydrogeological and damaged mountain environments of mines.

*Keywords:* Geological deformation; Numerical simulation; Environmental governance; Environmental impact assessment; Ecological restoration

---

### 1. Introduction

After mining the ore resources from underground, the raw equilibrium state was destroyed. The layer of the cover layer loses support, so the stress in the rock mass is reassigned [1] and the surface of GOF moves and deforms. When the mine reaches a certain range, movement and damage will spread to the surface [2]. This phenomenon is known in mining works as “mining settlement” [3]. The mine was abandoned. Mining settlement not only damages the

ecological environment, but also affects the stability of the structure and limits the sustainable development of mining [4]. This requires a lot of research on the hydrogeological movement and deformation of the abandoned mines. There are numerous abandoned mines due to long-unreasonable energy mining methods. Today, the ecological environment of abandoned landmines has been concerned about.

From “vertical line theory [5]” from Doris to 1838 proposed various applications with computers in the 21st century joint computers, mining subsidence theory research

---

\* Corresponding author.

has gone through a preliminary understanding and research stage, theoretical formation and rapid development by the study of Manuel Miguel et al. [6]. Nowadays, many domestic rock engineering numerical simulation software has appeared in succession, which has laid a solid foundation for the research of mining settlement. The hydrogeological mobile deformation assessment of the mine is mainly aimed at the impact of mining development on the environment. The method includes analytical hierarchical processing, fuzzy comprehensive evaluation, layer superposition method, setting pair analysis method, finite difference method and other methods, and some results are realized here [7].

We will investigate the hydrogeological mobility and environmental conditions of the abandoned mines. Then, the ground collapse rules and environmental treatment rules are studied. Using the combination of practical observations with numerical simulation by the study of Hao et al. [8], we study the mechanism of action and propose specific engineering control measures for possible problems.

## 2. Research method

### 2.1. Overview of the study area

After the mining process destroys the original balance of the mining area, the top strata will bend, move down, and even fracture and separate until the new balance is reached. In this process, various forms of deformation will occur, such as bending, caving, spalling, sliding, fracture, rock sliding along the plane, and uplift, as shown in Fig. 1.

In Fig. 1, a movable basin appears after the hydrogeological movement deformation of the abandoned mine, as shown in Fig. 2. During the formation of the surface moving basin, change the original surface shape, resulting in changes in height, slope, and horizontal position. Therefore, the roads, pipelines, canals, buildings and ecological environments in the affected areas will be affected to varying degrees.

The hydrogeological mining of an abandoned mine promoted rapid local economic and social development, but it occupied large amounts of cultivated land and woodland, polluted the environment, and thus needed to handle the local mine hydrogeological environment. In order to ensure

the effectiveness of the comprehensive mine environment management, it is necessary to conduct in-depth research and investigation on the hydrogeological environment background and existing problems of the mine, and to divide and evaluate the hydrogeological environment of the treatment area. The hydrogeological environment of abandoned mines in the area is mainly divided into open-pit mines and destructive mountains.

### 2.2. Surface deformation monitoring of the hydrogeology of an abandoned mine

#### 2.2.1. Monitoring instruments and equipment

TC402 total station is used to measure the horizontal displacement and trigonometric elevation of the monitoring point, and the static GPS (HD5800) receiver is used to monitor the datum point. Fig. 3 shows the instruments used in this survey.

The main technical specifications of the instrument are as follows. The model of TC402 Precision Total Station is Lecia TC402, the angle measuring accuracy is 2", and the distance measuring accuracy is 2 mm ± 2 ppm, the measurement time is 1 s, and the range is 3.0 km; the static GPS receiver of HD5800 is selected as the receiver, the horizontal and vertical displacement accuracy is ± (5 mm + 1 ppm), and the operating distance is 80 km.

#### 2.2.2. Layout of monitoring points

The subsidence area is selected as the best monitoring point. There are two working base points, namely, X0 and XN, where X0 is the assumed starting point and XN is the orientation point. The surface deformation monitoring points are arranged in the range of 3–5 km around the subsidence area above the original goaf. The quantity depends on the size of the collapse pit, and the distance between two adjacent points is about 20–30 m. Generally, concrete piles are used as monitoring marks. The monitoring points are arranged in the area with good field of vision, surrounding the working base points of X0 and XN. The monitoring points should be densely arranged in the direction of goaf, and the distance between other adjacent points should

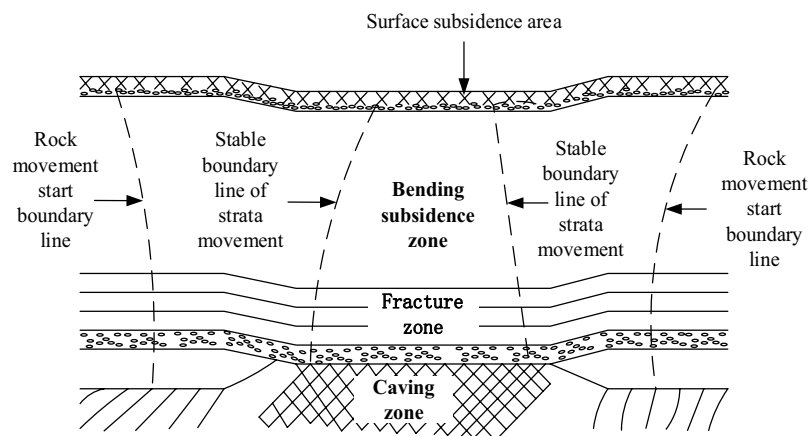


Fig. 1. Movement and deformation of overlying strata in an abandoned mine.

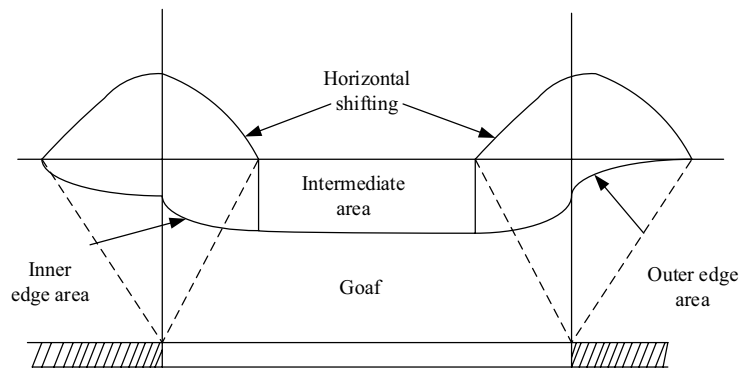


Fig. 2. The formation process of surface movement basin.



Fig. 3. Monitoring instruments (the figure on the left shows Leica TC402 Precision Total Station, and the figure on the right shows HD5800 Static GPS Receiver).

not exceed 50 m. Therefore, a total of 9 monitoring points, X1–X5 and X9–X12, are set up. A total of three deformation monitoring points X6–X8 are set between the +240 m contour line and the isolated pillar in the original collapse area, with the spacing of 15–20 m.

### 2.2.3. Survey method

The trigonometric leveling method is used to measure the elevation of X0 and each monitoring point. The elevation of each monitoring point uses the elevation of X0, and the method of trigonometric leveling is used for settlement observation of deformation monitoring points. The instrument is TC402 total station, and the distance between stations and points is kept within 50 m. In order to avoid the influence of atmospheric vertical refraction, the values are checked 2–3 times when values are read.

### 2.2.4. Determination of observation period

The surface deformation is a continuous and uneven process in time and space. However, the layout of surface monitoring points must be targeted and cannot be arranged in all directions. Similarly, it is intermittent in time, and the number of monitoring is limited. Therefore, it is very important to arrange the observation period properly.

The observation period of surface subsidence can be determined by the following empirical equation:

$$T \geq \sqrt{2} m_k \frac{K}{v} \quad (1)$$

where  $m_k$ : height error between two settlement observation points;  $v$ : the settlement velocity. It is generally the ratio of the average settlement to the interval day;  $K$ : the ratio of deformation value to its error. It can be selected from 5 to 10 according to the deformation of the monitored object.

## 2.3. Design and establishment of numerical simulation model

### 2.3.1. Numerical simulation analysis of geological movement and deformation of abandoned mine

With an abandoned mine as an example, the calculation model of ore body is built by Fast Lagrangian Analysis of Continua (FLAC3D) software to simulate the process of surface movement and deformation after excavation in different sections of the mining area, and the model is cut and analyzed.

According to the FLAC3D modeling method and the actual mine survey data, a three-dimensional model is established. The process is as follows. The coordinates are transformed, which makes the research simple, intuitive and convenient; according to the geological profile of the mine, the geometric model of the ore body is constructed; the ore body model is wrapped into a cuboid by surrounding rock blocks, and the divergent surrounding rock is established to form the geometric model of ore body surrounding rock.

The boundary conditions of the calculation model are as follows. The top of the model is set as a free boundary; the bottom boundary is constrained by displacement in the vertical direction, that is,  $u_z = 0$ ; the boundary of two end faces in  $x$ -direction of the model is constrained by displacement, that is,  $u_x = 0$ ; the boundary of the two end faces in the  $y$ -direction of the model is constrained by displacement, that is,  $u_y = 0$ ; the initial stress field of the model is automatically formed by the self-weight stress.

Then, the surrounding rock and ore body are regarded as isotropic elastic-plastic continuous medium, and the Mohr-coulomb yielding criteria is adopted for each filling body.

$$f_x = \alpha_1 - \alpha_3 \frac{1 + \sin \phi}{1 - \sin \phi} - 2c \sqrt{\frac{1 + \sin \phi}{1 - \sin \phi}} \quad (2)$$

where  $\alpha_1$  is the maximum principal stress,  $\alpha_3$  is the minimum principal stress,  $\phi$  is the friction angle and  $c$  is the cohesion. When  $f_x > 0$ , shear failure occurs on the material.

During the simulation, the model deformation is set to large deformation.

Three groups of monitoring points are set up, namely +150 m elevation, +190 m elevation, +230 m elevation, with 20 monitoring points in each group.

2.3.2. Hydrogeological environmental impact assessment of abandoned mine

The main environmental problems in the mine are open pit pits and damaged mountains. Environmental assessment will be divided into these two areas evaluate the hydrogeological environment of hydrogeological disasters and the distribution density through quantitative distribution.

The mathematical model is as follows: the fuzzy distinction of the distribution density of the mine hydrogeological environment problems.

The distribution density of the mine hydrogeological environment problems can be expressed as follows:

$$a_i = \frac{n}{s_1} \times 100 \tag{3}$$

where  $a_i$  is the distribution density of the  $i$  mine hydrogeological environment problem points (number/km<sup>2</sup> × 100)  $n$  is the number of mine geological environment problem points, and  $s$  is the area. The function (2) is used for fuzzy discrimination

$$A_i = \begin{cases} 0, & a_i = 0 \\ \frac{1}{1 + 25a_i^{-2}}, & 0 < a_i < 25 \\ 1, & a_i \geq 25 \end{cases} \tag{4}$$

where  $A_i$  is the fuzzy degree of distribution density of geological environment. The distribution density is greater than or equal to 25 is serious, and other less than 25 based (4).

The discrimination factor B of geological disaster is divided into two parts: unit property loss BB and distribution density BM of disaster points. The influence of potential geological disaster points is as important as the disaster points that have occurred, and the threat loss of dangerous situation is the same as the direct economic loss. It is also counted by 100 km<sup>2</sup>. Property loss per unit area is:

$$BB_i = \frac{\sum_{j=1}^n bbs_{ij}}{S_i} \times 100 \tag{5}$$

The distribution density of disaster points is as follows.

$$BM_i = \frac{m}{S_i} \times 100 \tag{6}$$

In Eqs. (5) and (6):  $bbs_{ij}$  is the property loss of geological disaster in area  $j$ ;  $m_i$  is the number of geological hazard points in area  $i$ . The classification table of geological hazard hazard degree in the code for risk assessment of geological hazards (DZ/T0286-2015) is taken as the reference. With 1 million

yuan and 5 million yuan as the classification standard, the hazard degree of geological hazard with more than or equal to 5 million yuan is large, and that with less than or equal to 1 million yuan is small. The fuzzy discriminant function (7) is established as follows:

$$CC_i = \begin{cases} \frac{CC_i}{100} \times 0.1, & cc_i \leq 100 \\ 0.1 + 0.9 \times \frac{cc_i - 100}{500 - 100}, & 100 < cc_i < 500 \\ 1, & cc_i \geq 500 \end{cases} \tag{7}$$

In Eq. (5), CC is the fuzzy attribution degree of property loss per unit area. If the property loss per unit area is more than or equal to 5 million yuan/km<sup>2</sup>, the serious attribution degree is 1, and if the property loss per unit area is less than 5 million yuan/km<sup>2</sup>, Eq. (5) is used to judge.

And take the hydrogeological hazard risk assessment specification and the geological disaster degree classification table as a reference, as shown in Fig. 4.

According to the hydrogeological disaster degree classification table shown in Figs. 4 and 5 small disasters can be taken as 1 large disaster. In order to increase its convergence, the distribution density of disaster points is increased by 10 times, and the fuzzy discriminant function (8) of distribution density of disaster points is established.

$$CM_i = \begin{cases} 0, & b_i = 0 \\ \frac{1}{1 + 50(10cm_i)^{-2}}, & 0 < b_i < 5 \\ 1, & b_i \geq 5 \end{cases} \tag{8}$$

$CM_i$  is the fuzzy attribution degree of distribution density of disaster points. If the density of the problem point is greater than or equal to 5, it is serious. If it is less than 5, the fuzzy judgment can be made by Eq. (6). The fuzzy discriminant function (9) is established as follows:

$$C_i = 0.5 \times CC_i + 0.5 \times CM_i \tag{9}$$

The fuzzy discriminant matrix  $R_{ij}$  is established. According to the above functions, the attribution of the impact severity of the mine hydrogeological environment can be calculated, and the fuzzy discriminant matrix  $R_{ij}$  is established:

$$R_{ij} = \begin{Bmatrix} A_1 & B_1 & C_1 \\ A_2 & B_2 & C_2 \end{Bmatrix} \tag{10}$$

$i$  is divided into 1 and 2 regions;  $j$  is A, B, and C.

This matrix is introduced to determine the severity of the mine hydrogeological environment impact.

$$R_\lambda = (R_{ij}^\lambda)_{m \times n} \tag{11}$$

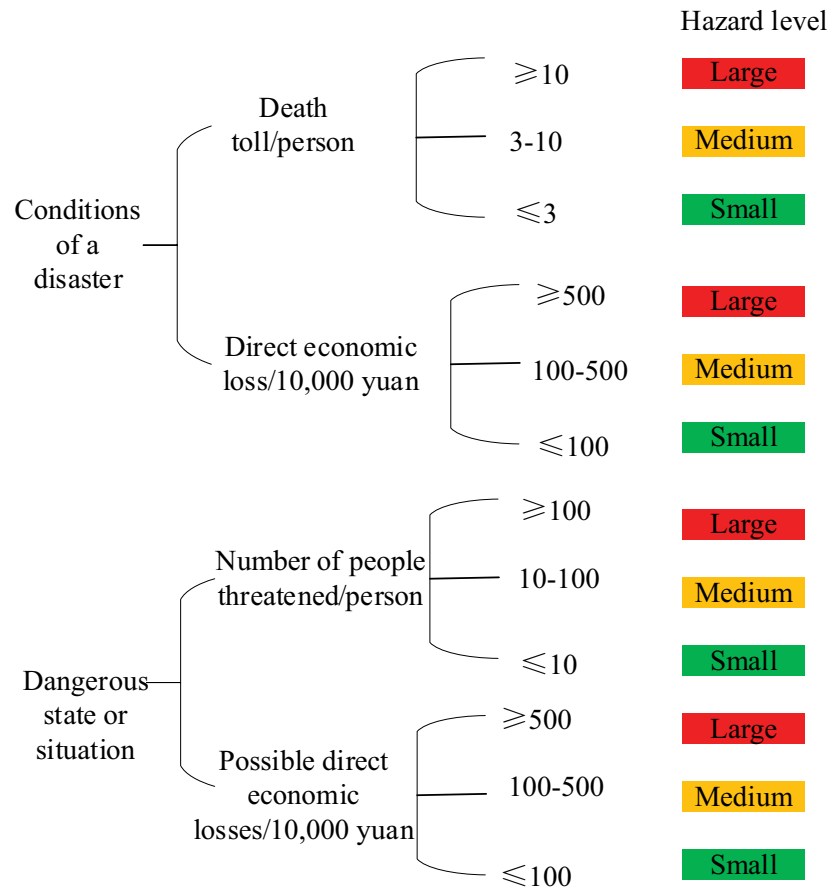


Fig. 4. Classification table of geological hazard degree.

$\lambda = 0.9, 0.5$  and  $0.1$  are taken respectively for judgement. R0.9 is classified as severe area, R0.5 without R0.9 is classified as relatively severe area, R0.1 without R0.5 is classified as mild area, and R0.1 is classified as general area.

### 3. Results and discussion

#### 3.1. Monitoring results of the hydrogeological movement and deformation of the spoil mine

According to the detection requirements, from March 2020 to March 2021, the surface around the mine collapse pit is measured for seven times. The measurement dates are 2020.03.09, 2020.04.28, 2020.07.15, 2020.08.23, 2020.09.17, 2020.12.14 and 2020.03.09, respectively. The hydrological surface deformation monitoring cycle of an abandoned mine is as follows. Settlement observation and monthly observation level movement, and working base points are measured every six months. The monitoring result is Fig. 5.

The monitoring results in Fig. 5 show that the X, Y and Z coordinates have little change. The maximum cumulative offset of X coordinates is X4 point, with a cumulative offset of  $-27$  mm, and the minimum is X8 point, with a cumulative offset of  $3$  mm; the maximum cumulative offset of Y coordinate is X5 point, with a cumulative offset of  $-35$  mm, and the minimum is X11 point, with a cumulative offset of  $2$  mm; the Z coordinate also changes slightly in this monitoring.

The point with maximum accumulated settlement is X7, with the accumulated settlement of  $-13$  mm, and the point with maximum accumulated settlement is X4, with the accumulated settlement of  $-1$  mm.

It suggests that the accumulated horizontal displacement of the mine is gradually increasing, and the accumulated settlement displacement is basically unchanged, which indicates that the settlement is basically stable, the horizontal movement is relatively active, and the mine is prone to landslide, collapse and other hazards. Risk factors of such hydrogeological hazards can be reduced by controlling the environment around the mine.

#### 3.2. Mechanical parameters of model medium

The mechanical parameters of the model are determined by analogy method with reference to similar mines. Fig. 6 presents the specific data of mechanical parameters of the three main rocks. The main mechanical parameters of rock include density, elastic modulus, Poisson's ratio, cohesion, uniaxial tensile strength and internal friction angle.

#### 3.3. Settlement analysis

After the excavation of  $x = +125$  m horizontal ore body, Figs. 7 and 8 are the vertical sections of the settlement, and the sections are  $y = +220$  m and  $y = +260$  m respectively.

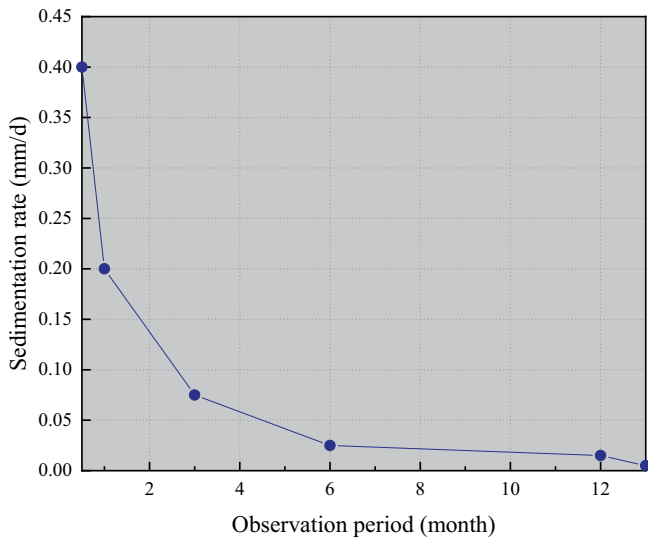


Fig. 5. Settlement observation data.

The section in Fig. 7 suggests that  $y = +220$  m, the main settlement is located between  $x = 160$  m and  $x = 240$  m above the hollow area of the section, which is inferred to be caused by the large span of the hollow area of the section.

Fig. 8 shows that the maximum roof settlement value is 1.48 mm, which is located between  $x = +120$  m and  $x = +240$  m directly above the hollow area of  $y = +260$  m profile. It is inferred that it is caused by the large span of hollow area of profile. The color change is uniform above the  $y = +220$  m and  $y = +260$  m profile goaf, indicating that the settlement of the strata above the area is more uniform and regular.

Figs. 9 and 10 present the cloud atlas of subsidence of the horizontal section of  $z = +165$  m and  $z = +205$  m in computer simulation. According to the analysis of Fig. 9, when  $z = +165$  m, the maximum deposition area of roof is concentrated between  $x = +120$  and  $x = +150$ , and between  $y = +240$  m and  $y = +270$  m, and the range of settlement value in this area is 1.4–1.48 m.

Fig. 10 shows that when  $z = +205$  m, the maximum deposition area of the roof is concentrated between  $x = +115$  and  $x = +140$ , and between  $y = +245$  m and  $y = +265$  m, with the range of settlement value of 1.1–1.13 m.

Fig. 11 is a cloud atlas of surface subsidence. The maximum settlement area is concentrated between  $x = +100$  and  $x = +140$ , and between  $y = +245$  m and  $y = +270$  m. The range of settlement value in this area is 0.55–0.59 m. The analysis of model diagram in Figs. 9–11 show that the settlement of horizontal section at +125 m elevation is the largest, the surface settlement is the smallest, and the shape after settlement is similar. The maximum surface subsidence is 0.59 m.

Fig. 12 shows the monitoring settlement curve of three monitoring points at  $x = +205$  m elevation, +165 m elevation and +125 m elevation. The curve chart of monitoring results shows that the change range of settlement curves of +205 m, +165 m, and +125 m monitoring points is similar. Among them, the 12th monitoring point has the largest settlement value. The value of the first three monitoring points are smaller and the curve is slower. From the fourth point, the settlement value increases obviously. Until the twelfth

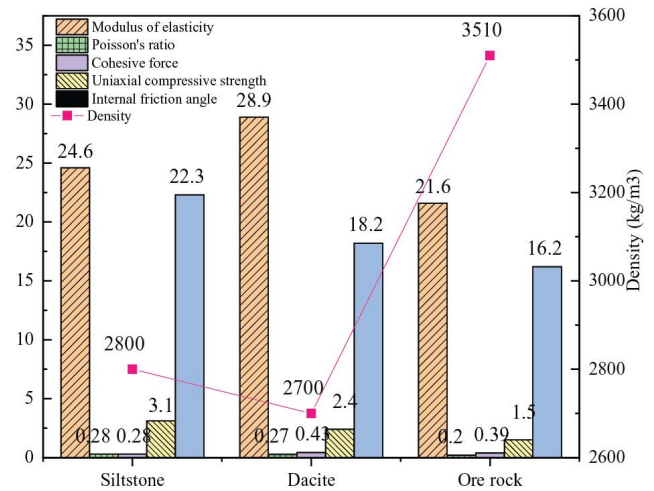


Fig. 6. Mechanical parameters of the model.

point, the settlement value begins to decrease. The settlement value from point 13 to point 20 is small and the curve is slow.

The software simulation and settlement analysis reveal that the mountain subsidence degree of the abandoned mine is not large, but many small low-lying terrains has been formed, which is very likely to further develop into a mined gob basin, and has a great impact on the environment.

### 3.4. Horizontal displacement analysis

According to the analysis of FLAC3D software, the displacement cloud atlas of the abandoned mine in x-axis direction and y-axis direction is given, as shown in Figs. 13 and 14. Figs 13 and 14 show that the maximum displacement of the surface in the positive x direction is 0.168 m, and that in the negative x direction is -0.197 m. There are two obvious areas of surface movement, which are regular in shape and semi-circular. It indicates that after the excavation of the ore body, the surface gradually sinks, forming regular pits, and the soil or rock at the edge of the pits gradually moves towards the pits, or even dumps into the pits. The obvious surface movement area is mainly concentrated in the edge of the pit, and the horizontal movement inside the pit is not obvious. The maximum displacement in the positive direction of y is 0.226 m, and the maximum displacement in the negative direction is -0.197 m. Compared with x, the maximum displacement in y direction increases obviously. Similarly, the obvious area of surface movement is also concentrated on the edge of the surface pit, and the horizontal movement inside the pit is small.

According to the horizontal displacement analysis, the displacement along X axis, Y axis and Z axis is small, and the movement range is not large. It will not easily cause landslide and other geological disasters. If the vegetation coverage around the ore body is not enough, landslide may occur.

### 3.5. Environmental assessment results and ecological restoration

The evaluation results show that most of the mines in this area are slightly affected areas, with an area of

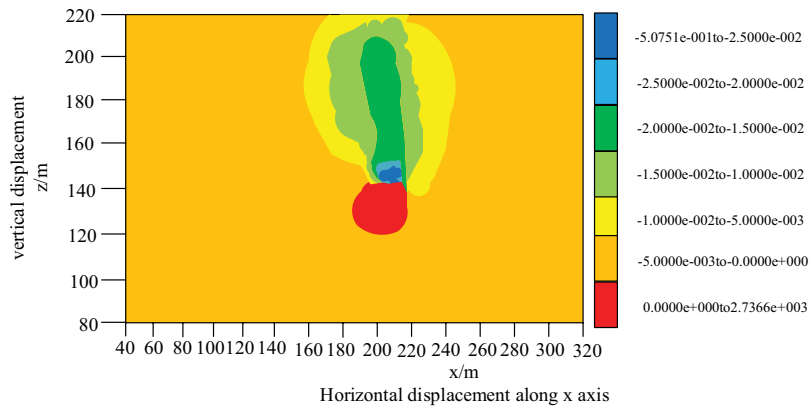


Fig. 7. Section of  $y = +220$  m.

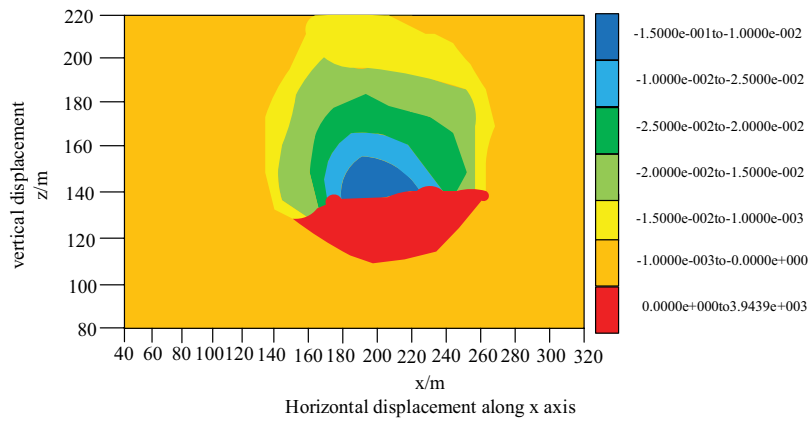


Fig. 8. Section of  $y = +260$  m.

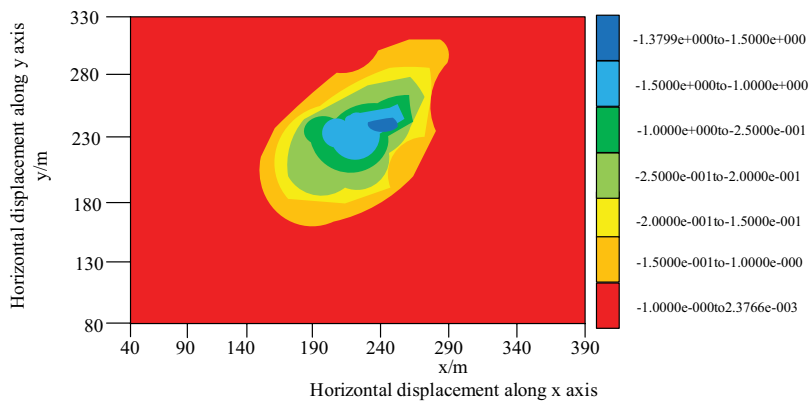


Fig. 9. Settlement cloud atlas of  $z = +165$  m horizontal section.

219.14 km<sup>2</sup>, and a few are relatively serious areas, with an area of 53.78 km<sup>2</sup>.

Open pit: the recoverability of the land area occupied by open pit is relatively poor, and the recovery difficulty and capital investment are relatively large. Many pits are about 3 m deep and have accumulated water, so deep excavation and shallow bedding can be considered to reclaim them into cultivated land or woodland. For some deep-water pits, it can be considered to be converted into fishery pond according to

their water quality [9]. In addition, protective net and safety warning signs shall be set up beside the pit to prevent the safety of surrounding residents from being threatened.

Damaged mountain: it can be considered to restore to woodland [10]. Clearing dangerous rocks, backfilling planting soil, planting saplings and other measures can be taken for mine greening and improving the regional natural environment, or the damaged mountain can be rebuilt into construction land [11,12].

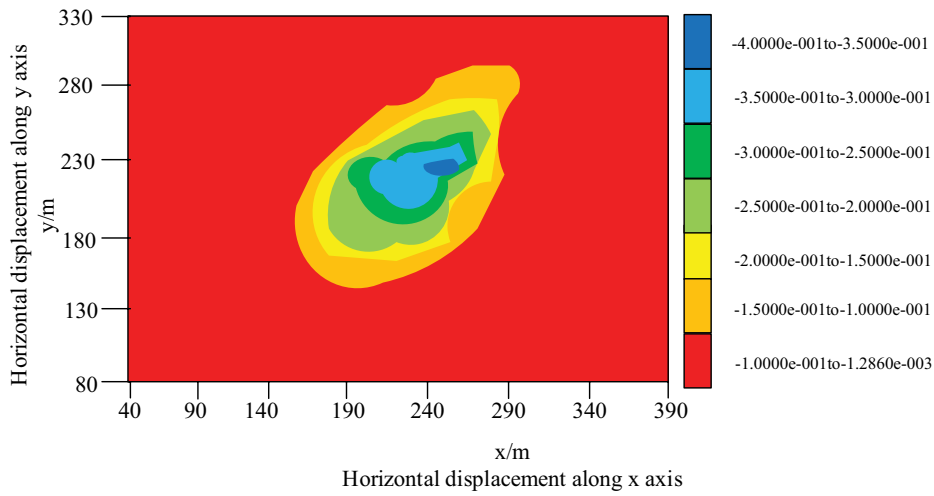


Fig. 10. Settlement cloud atlas of horizontal section of  $z = +205$  m.

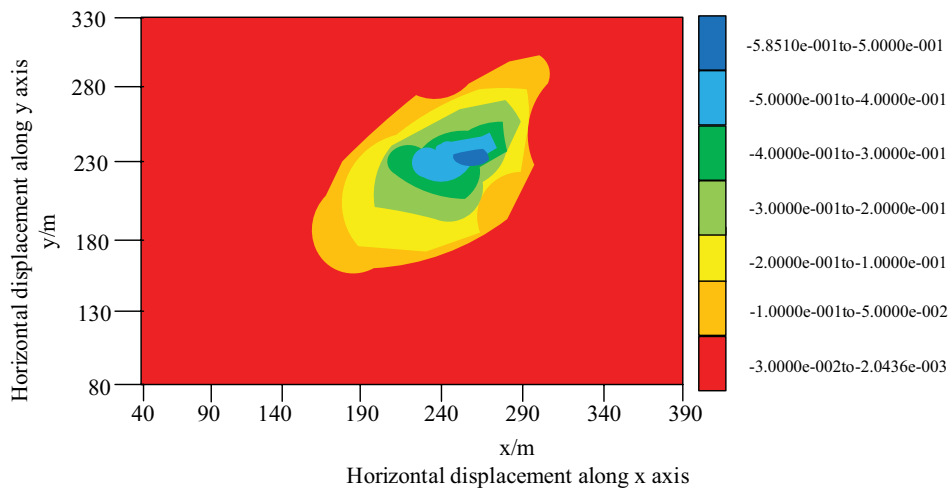


Fig. 11. Cloud atlas of surface subsidence.

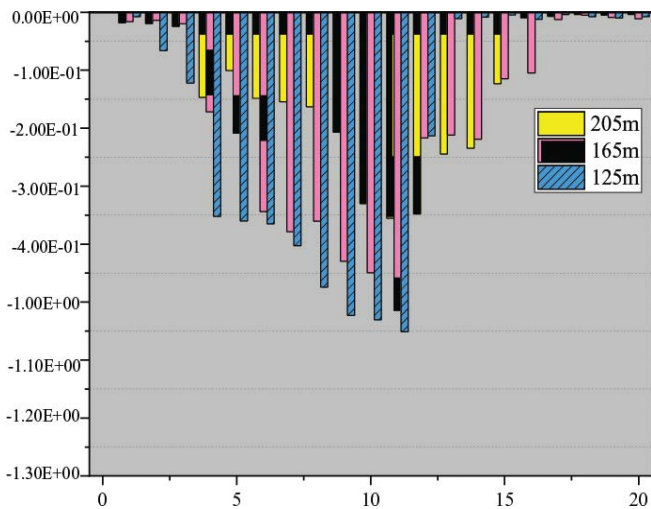


Fig. 12. Settlement curve of monitoring points.

Open pit and damaged mountain need vegetation coverage, in order to effectively reduce the occurrence of geological disasters. The reconstruction of abandoned mines is also an effective way to achieve waste utilization [13].

#### 4. Conclusion

Based on the basic law of surface subsidence, the motion process of abandoned geology and its influence on the surface are analyzed. Monitor the ground surface around the collapse pit. Monitoring results showed that the surface settlement is more stable, and the horizontal movement is more active. Numerical simulation analysis of the mine is performed with FLAC three-dimensional software. Excavation results show that the surface settlement is the obvious maximum, and the top of the model is bent downward, indicating that the surface may form a sunken basin. The environmental problems of abandoned mines are mainly divided into open-pit mines and destructive mountains.

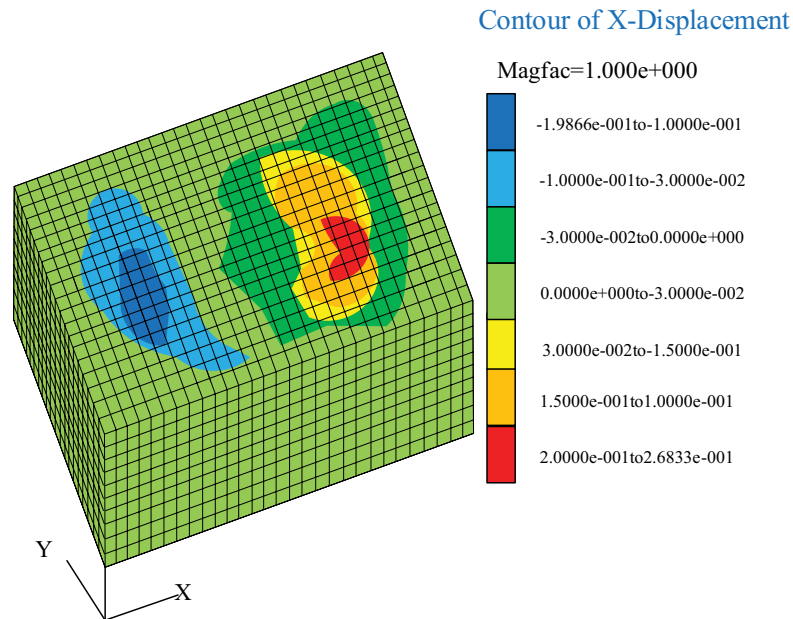


Fig. 13. Displacement cloud atlas in the  $x$ -direction.

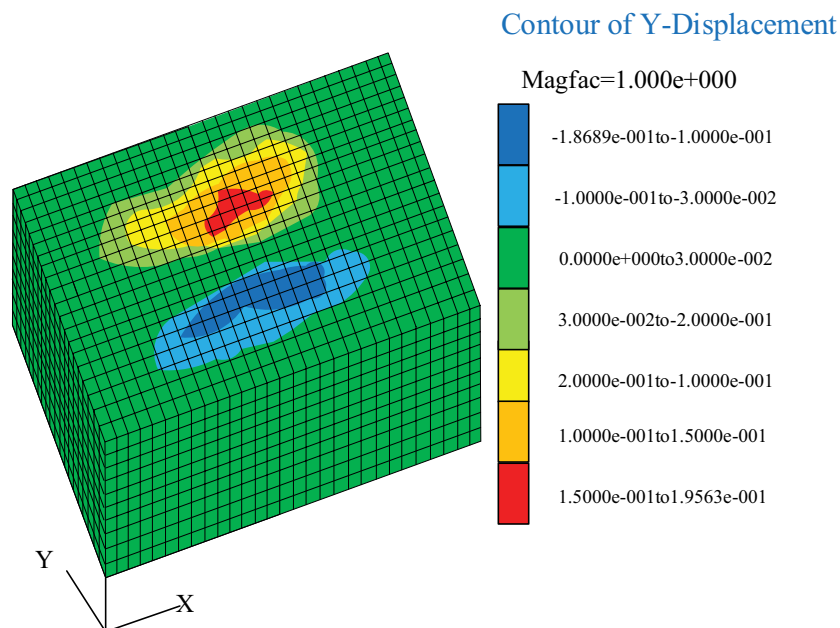


Fig. 14. Displacement cloud atlas in the  $y$ -direction.

The hydrogeological environment impact assessment of the mine is divided into two areas: the area with serious environmental impact and the area with slight hydrogeological environment impact. Based on this, suggestions are made on the environmental protection and restoration of the hydrogeology of abandoned mines. According to the actual situation, the abandoned mines can be converted into woodland, cultivated land and grassland.

#### References

- [1] F.F. Martins, G. Vasconcelos, T. Miranda, Prediction of the mechanical properties of granites under tension using DM techniques, *Geomech. Eng.*, 15 (2018) 631–643.
- [2] A. Nwachukwu, H. Jeong, M. Pyrcz, L.W. Lake, Fast evaluation of well placements in heterogeneous reservoir models using machine learning, *J. Pet. Sci. Eng.*, 163 (2018) 463–475.
- [3] R. Prasad, K.D. Yadav, Use of response surface methodology and artificial neural network approach for methylene blue

- removal by adsorption onto water hyacinth, *Water Conserv. Manage.*, 4 (2020) 79–85.
- [4] S.M. Al-Gorany, S.Z. Al-Abachi, A.I. Arif, E.E. Aboglid, E.H. Al-Abdeli, Preliminary phytochemical screening and GC-MS analysis of bioactive constituents in the ethanolic extract of empty fruit bunches, *J. Clean WAS*, 4 (2020) 70–74.
- [5] A. Kolapo, C.F. Ojo, A.M. Lawal, T.S. Abayomi, O.A. Muhammed, Sensitivity analysis and future farm size projection of bio-fortified Cassava Production in Oyo State, Nigeria, *J. Sustainable Agric.*, 5 (2021) 61–66.
- [6] J.V. Manuel Miguel, E. García-Sánchez, M.B. Almendro-Candel, A.B. Vicente, T. Sanfeliu, J. Bech, Technosols designed for rehabilitation of mining activities using mine spoils and biosolids, *Catena*, 14 (2017) 74–80.
- [7] Z.-q. Li, Y.-g. Xue, S.-c. Li, L.-w. Zhang, D. Wang, B. Li, W. Zhang, K. Ning, J.-y. Zhu, Deformation features and failure mechanism of steep rock slope under the mining activities and rainfall, *J. Mountain Sci.*, 14 (2017) 54–58.
- [8] Y. Hao, Y. Wu, P.G. Ranjith, K. Zhang, H. Zhang, Y. Chen, M. Li, P. Li, New insights on ground control in intelligent mining with Internet of Things, *Comput. Commun.*, 150 (2020) 788–798.
- [9] C. Newman, Z. Agioutantis, N. Schaefer, Development of a web-platform for mining applications, *Int. J. Mining Sci. Technol.*, 28 (2018) 78–82.
- [10] S. Zhao, F. Liu, P. Yang, H. Zhao, A. Asundi, L. Yan, H. Zhao, Microlens light field imaging method based on bionic vision and 3-3 dimensional information transforming, *J. Geodesy Geoinf. Sci.*, 2 (2019) 33–36.
- [11] A. Punia, P.K. Joshi, N.S. Siddaiah, Characterizing Khetri copper mine environment using geospatial tools, *SN Appl. Sci.*, 3 (2021) 1–17, doi: 10.1007/s42452-021-04183-6.
- [12] S. Liu, Y. Shi, M. Feng, Routing design and experimental analysis of wireless sensor monitoring network for mine environment, *J. Comput. Methods Sci. Eng.*, 20 (2020) 609–620.
- [13] Z. Sawłowicz, L. Malinowski, A. Giż, J. Stanek, J. Przybyło, Mineralogical-geochemical study of corroded iron-based metals from a salt mine environment, *Corrosion*, 76 (2020) 666–677.